Hydrol. Earth Syst. Sci. Discuss., doi:10.5194/hess-2016-93, 2016
Manuscript under review for journal Hydrol. Earth Syst. Sci.
Published: 4 March 2016

Hydrology and Earth System Sciences
Discussions

Repeated electromagnetic induction measurements for mapping soil moisture at the field scale: validation with data from a wireless soil moisture monitoring network

Edoardo Martini[1], Ulrike Werban[1], Steffen Zacharias[1], Marco Pohle[1], Peter Dietrich[1,2] and Ute Wollschläger[3]

[1] Dept. Monitoring and Exploration Technologies, UFZ - Helmholtz Centre for Environmental Research, Permoserstraße 15, 04318 Leipzig, Germany.
[2] Centre for Applied Geoscience, University of Tübingen, Hölderlinstraße 12, 72074 Tübingen, Germany.
[3] Dept. Soil Physics, UFZ - Helmholtz Centre for Environmental Research, Theodor-Lieser-Straße 4, 06120 Halle (Saale), Germany.

Correspondence to: E. Martini (edoardo.martini@ufz.de)

Abstract

Electromagnetic induction (EMI) measurements are widely used for soil mapping, as they allow fast and relatively low-cost surveys of soil apparent electrical conductivity (ECa). Although the use of non-invasive EMI for imaging spatial soil properties is very attractive, the dependence of ECa on several factors challenges any interpretation with respect to individual soil properties or states such as soil moisture (θ). The major aim of this study was to further investigate the potential of repeated EMI measurements to map θ, with particular focus on the temporal variability of the spatial patterns of ECa and θ. To this end, we compared repeated EMI measurements with high-resolution θ data from a wireless soil moisture and soil temperature monitoring network for an extensively managed hillslope area for which soil properties and θ dynamics are known. For the investigated site, i) ECa showed small temporal variations whereas θ varied from very dry to almost saturation; ii) temporal changes of the spatial pattern of ECa differed from those of the spatial pattern of θ; and iii) the ECa-θ relationship varied with time. Results suggest that i) stable soil properties are the major control on ECa measured with EMI, and ii) for soils with low clay content, the electrical conductivity of the soil solution rather than θ is likely to be the dynamic factor controlling temporal variations of ECa. Further, our study provides the opportunity to discuss the complex interplay between factors controlling ECa and θ, and the use of EMI-based ECa data with respect to hydrological applications.

1 Introduction

Electromagnetic induction (EMI) methods are widely used for soil mapping, as they allow fast and relatively low-cost surveys of soil apparent electrical conductivity (ECa) over areas up to several km^2 in size (McNeil, 1980). The main strength

Hydrol. Earth Syst. Sci. Discuss., doi:10.5194/hess-2016-93, 2016
Manuscript under review for journal Hydrol. Earth Syst. Sci.
Published: 4 March 2016

of the EMI method is that the induction principle does not require a direct contact with the ground. Consequently, a survey carried out using EMI sensors can be accomplished faster than an equivalent survey carried out with other instruments. Normally, surveys can be performed by a single operator, and a GPS receiver connected to the instrument allows collecting georeferenced ECa data. Measurements of ECa using EMI are in use since the 1970's, initially having been developed for applications related to soil salinity. Since then, various environmental questions have been addressed using the EMI method, as discussed in the recent review of Doolittle and Brevik (2014). Although the use of non-invasive geophysical techniques for soil mapping is very attractive, the dependence of ECa on a number of parameters complicates any interpretation to determine soil properties or states (Robinson et al., 2012). A firm understanding of the spatial and temporal variability of soil electrical conductivity (EC) and an appreciation for its highly complex interactions with static and dynamic soil properties, particularly at low-salt concentrations, is needed (Sudduth et al., 2001; Sudduth et al., 2005; McCutcheon et al., 2006), and it is helpful for understanding when EMI can be applied, as it is not applicable under all circumstances (Robinson et al., 2012).

The theory and basic principle of EMI-based measurements of ECa refers to the mechanistic soil ECa model proposed by Rhoades et al. (1989), which is based on the soil equivalent resistance model (Sauer et al., 1955). Soil ECa is assumed to arise from three conductance pathways through the soil: i) a conductance pathway traveling through a continuous soil solution, ii) a conductance pathway traveling through the solid particles, and iii) an alternating solid-liquid pathway (Rhoades et al., 1989). In this formulation, the total soil water content is separated into the fraction of water content in the fine pores (mostly adsorbed by the clay minerals, contributing to the alternating solid-liquid pathway) and the water content in the large pores (which contributes to the continuous liquid pathway). The soil ECa is influenced by the volumetric content (θ), the EC of the fractions of soil solution (EC_w), as well as by the volume of the solid particles and their EC (EC_s). As a consequence, several factors influence ECa (Friedman, 2005). To a higher clay content and/or higher organic matter content usually correspond a higher content of adsorbed water (i.e., higher θ), higher EC_s, and higher cation exchange capacity (CEC, which in turn has the potential to increase the EC_w), thus leads to higher ECa. Moreover, of particular importance is EC_w, which often increases with higher CEC, as ions can be released into the soil solution. In this respect, the initial EC of rain water, its residence time in the soil and the mineralogical composition of the soil play a role. Soil compaction affects ECa due to the reduced porosity and increased soil particle-to-particle contact (Corwin et al., 2008). Soil temperature also affects ECa, which increases approximately 1.9 % per degree centigrade (USDA, 1954; Corwin and Lesch, 2005). All these mechanisms contribute to the complexity of ECa and soil property relationships. Corwin et al. (2008) and Farahani et al. (2005) highlighted that the ECa versus soil property functions are expected to be temporally variable unless EC_w and θ remain relatively unchanged, assuming EC_s to be stable at the temporal scale of observation.

In the last decades, a number of sensors were developed for field measurements of ECa, based on the electromagnetic induction principle. Technically, a transmitter and a receiver coil are placed on (or near) the soil surface at a fixed distance from each other, and the transmitter coil is energized with an alternating current. This generates a time-varying magnetic field, which induces electric fields in the soil, which in turn induce a secondary magnetic field. Such phenomena are described by Ampere's and Maxwell's laws. Both the primary and the secondary magnetic fields are sensed by the receiver

Hydrol. Earth Syst. Sci. Discuss., doi:10.5194/hess-2016-93, 2016
Manuscript under review for journal Hydrol. Earth Syst. Sci.
Published: 4 March 2016

coil and, under certain geometric conditions indicated as "low induction number" (McNeill, 1980; Callegary et al., 2007; Callegary et al., 2012), the ratio between the primary and the secondary magnetic field can be used to estimate the ECa of the volume of soil under investigation. As the final reading refers to a certain volume of soil material, it is indicated as apparent electrical conductivity ECa. Several factors influence the physical process described above. As the intercoil spacing *s* increases, the EM field propagates through a larger volume of soil. As the operating frequency increases, the EM field is more attenuated and therefore penetrates less into the soil, reducing the volume of investigation. Transmitter and receiver coils are commonly adjusted in coplanar configuration. Vertical coplanar coils (VCP) generate horizontal magnetic dipole orientation (HDP), whilst the horizontal coplanar coil configuration (HCP) generates a vertical magnetic dipole (VDP). The coil configuration has implications for the volume of investigation. McNeill (1980) provided the relative response versus depth for an EMI device in both HDP and VDP and the "cumulative response" for homogeneous and layered soils. According to that, the response of an EMI device in HDP has larger sensitivity close to the soil surface (or, more precisely, immediately below the coils), with monotonic decay with depth, whilst the VDP configuration provides maximum sensitivity to the depth of ca. $0.4 \cdot s$ (i.e., 40% of the intercoil spacing). Additionally, the effective depth of exploration, defined as the portion that contributes with 70% to the measured value of ECa, is $0.75 \cdot s$ for the HDP and $1.50 \cdot s$ for the VDP configuration. Callegary et al. (2007 and 2012) discussed these concepts using a forward model of electromagnetic field propagation, and found that the sensitivity of any EMI sensor to soil ECa as well as the depth of investigation can differ significantly from those suggested by McNeil (1980). Nevertheless, it appears clear that the final ECa reading of any EMI device is a complex physicochemical measurement which results from the propagation of the EM field within the volume of investigation and its interaction with stable and transient soil properties/states, and that the effective measurement depth and volume of investigation of an EMI sensor may vary at different times and locations (Sudduth et al., 2001; Corwin and Lesch, 2005; Farahani et al., 2005; Callegary et al., 2007; Corwin et al., 2008; Werban et al., 2009; Zhu et al., 2010; Robinson et al., 2012; Callegary et al., 2012).

The fact that ECa measured with EMI responds to variations of several soil properties encouraged its use for a broad range of scopes. Examples of the application of EMI-based ECa measurements include soil salinity (e.g., Doolittle et al., 2001), spatial pattern of soil texture (e.g., Abdu et al., 2008), lateral boundaries between soil types (e.g., James et al., 2003), depth to clay-rich layers (e.g., Saey et al., 2009), clay content (e.g., Weller et al., 2007), soil compaction (e.g., Al-Gaadi, 2012), soil CEC (e.g., Triantafilis et al., 2009), soil organic carbon (e.g., Martinez et al., 2009; Werban et al., 2009; Altdorff et al., 2016), assessment of soil quality (e.g., Corwin and Lesch, 2005), detection of buried services (e.g., El-Quady et al., 2014), and mapping of active layer thickness in permafrost areas (e.g., Dafflon et al., 2013). ECa is widely used in the context of precision agriculture for, e.g., refining existing soil maps (e.g., Martini et al., 2013), precision farming (e.g., Lück et al., 2009; Scudiero et al., 2015) and harvest zoning (e.g., Priori et al., 2013).

EMI has become widely used to determine soil water content or to study hydrological processes within the field of hydrogeophysics (Binley et al., 2015). In a recent work, Calamita et al., (2015) listed 20 of the papers which address the use of EMI sensors for the determination of spatial and temporal patterns of θ. This summary provides a clear illustration of the

Hydrol. Earth Syst. Sci. Discuss., doi:10.5194/hess-2016-93, 2016
Manuscript under review for journal Hydrol. Earth Syst. Sci.
Published: 4 March 2016

Hydrology and Earth System Sciences
Discussions

differences among ECa-θ studies: estimation of θ was attempted for different soils and under varying climatic conditions, from the plot to the small catchment scale, with different temporal resolutions, and with different measurement schemes. The temporal resolution varied between one measurement date up to several days or years. Soil water content was estimated with a variety of probes down to different depths of the soil profiles and sometimes total water storage down to a certain soil depth was inferred. However, discrepancies exist between the depth of soil moisture measurements and the theoretical investigation depth of the EMI sensor in use. For most of the studies discussed in Calamita et al. (2015), ECa was measured with EM38 (Geonics Ltd., Canada), which is in fact the most widely used EMI sensor.

Because factors affecting ECa readings are complex and often interrelated, accurate interpretations have been a challenge (Zhu et al., 2010). In particular, the transient nature of soil water content and soil temperature was found to complicate the characterization of ECa variability by altering its response to a given soil property during a given mapping event (McCutcheon et al., 2006), such that the spatial and temporal variance of θ explained by EMI-ECa data is strongly unstable (Calamita et al., 2015). Repeated EMI measurements at one site (which require accounting for temperature changes between different dates) allow inferring the dynamic component of the signal, based on the assumption that changes of ECa are related to changes in the volume of water in the soil pores and/or changes in the concentration of ions in the soil solutions.

Zhu et al. (2010) conducted repeated EMI measurements under varying moisture conditions on a 19.5 ha agricultural field in Central Pennsylvania, and found that the spatial pattern of standardized ECa remained relatively stable over time. In their study, the R^2 values between ECa and θ measured at different depths varied between 0.24 and 0.47. The authors argued that, because of the spatial variability of soil and hydrologic properties across the landscape, "the effect of soil moisture on ECa could have been masked by other variations of soil properties and terrain attributes". Soil ECa was strongly influenced by soil moisture during wetter periods and at wetter locations, whilst other factors masked the effect of soil moisture on ECa variations during drier periods and at drier locations. They also remarked that the relationship between temporal variations of the soil ECa and soil water dynamics has not been thoroughly investigated for different soil moisture conditions and drying–wetting cycles, because simultaneous soil moisture measurements and EMI surveys were conducted only three times in this study.

Martinez et al. (2010) measured soil ECa during 13 occasions over three years in Vertisols to map temporal changes of the spatial pattern of θ. They used a principal component analysis to detect the main sources of variation of ECa, and found that the EM38-DD could successfully identify changes in soil properties due to tillage (i.e., changes of soil porosity) and formation of cracks within the soil profile. In fact, the first three components (90% of the ECa variability explained) were related to soil spatial variability, soil management, and topography. Soil water dynamics reflected temporal variations of the above mentioned factors, and could therefore be identified only as a less important signal.

Robinson et al. (2012) conducted EMI measurements on 9 occasions within five months in a small forested catchment with contrasting soil textures. Similar to the finding of Western et al., 2003, they found that two distinct patterns are present in the ECa and modelled θ maps: in the wet state, the spatial pattern of ECa correlated well with the spatial pattern of clay content, which, in turn, correlated well with θ, whilst the pattern in the dry state shows a smaller degree of organization and

Hydrol. Earth Syst. Sci. Discuss., doi:10.5194/hess-2016-93, 2016
Manuscript under review for journal Hydrol. Earth Syst. Sci.
Published: 4 March 2016

reasonable uniformity in θ across the catchment. They proposed a differencing approach to estimate θ from ECa, which improved the correlation from R^2 = 0.28 to R^2 = 0.48.

Recently, Shanahan et al. (2015) used repeated EMI measurements and electrical resistivity tomography to model soil EC, combined with laboratory estimates of gravimetric soil water content (θ_g), to investigate more specifically the effects of θ on EC in soils with contrasting texture and under different wheat genotypes. They documented difficulties of relating soil EC to θ_g; in fact, they observed that the correlation between changes in soil EC and changes in θ_g varied with time and that the correlation was better for the investigated loamy sand soil than for the clay loam that was also investigated by them. The authors concluded that in soils where the effect of EC_w appears to be larger, "changes in bulk EC, measured by EMI, may be confounded by increased pore water conductivity and less closely associated with changes in θ_g".

Findings of the studies summarized above show clearly the need for a more in-depth examination of the ECa-θ relationship for soils under field conditions, with specific attention to the physical principles controlling the EMI measurements. This study aims to further investigate the potential of repeated EMI measurements with wide spatial coverage to capture field-scale soil water dynamics. To this end, we compare time series of EMI measurements with high-resolution data from a wireless soil moisture and soil temperature monitoring network for a hillslope area in the Schäfertal catchment (Harz Mountains, Central Germany) for which spatial soil properties and soil moisture dynamics are known in detail. This gives us the opportunity to discuss the complex interplay between factors controlling ECa and θ, and the use of EMI-based ECa data with respect to hydrological applications.

2 Material and methods

2.1 Site description

The study was carried out on a hillslope at the Schäfertal experimental site, a small headwater catchment (1.44 km^2) located in the Lower Harz Mountains, Central Germany (51°39'N, 11°03'E) (Borchardt, 1982; Reinstorf et al., 2010a; Martini et al., 2015). The Schäfertal is a highly instrumented intensive research catchment within the TERENO "Harz/Central German Lowland Observatory" (Zacharias et al., 2011; Wollschläger et al., submitted).

The catchment receives an average precipitation of 630 mm per year (of which a large fraction may be falling as snow, according to the annual winter conditions) and has an average annual air temperature of 6.9°C with a subcontinental superimposed climate (Reinstorf et al., 2010b). The slopes of the Schäfertal catchment are formed by Devonian argillaceous shales and greywackes of the so-called Tanner Zone, which are covered by periglacial sediments (Borchardt, 1982). Cambisols and Luvisols are the dominant soil types on the slopes of the catchment, and Gleysols occupy the valley bottom (e.g., Ollesch et al., 2005). Interflow is known to play a relevant role within the runoff processes (Borchardt, 1982), and part of it can result in return flow. The slopes of the catchment are intensively used for agriculture, whilst meadow occupies the valley bottom (Schröter et al., 2015).

Hydrol. Earth Syst. Sci. Discuss., doi:10.5194/hess-2016-93, 2016
Manuscript under review for journal Hydrol. Earth Syst. Sci.
Published: 4 March 2016

The hillslope site investigated for this study is a grassland transect beside the agricultural fields at the outlet of the catchment and consists of a north and a south exposed slope and a valley bottom where the creek Schäferbach lies (Figure 1). The spatial extent is ca. 250 m by 80 m. The detailed soil mapping for the Schäfertal hillslope site is described in Martini et al. (2015) and revealed low textural variations. The site is extensively managed, i.e. neither irrigation nor fertilizers are applied, which might alter EC_w and effect ECa. Data from TERENO SOILCan lysimeters (Pütz et al., 2011) located within the south-exposed slope of the study area indicate ECw < 0.10 mS/cm throughout the monitoring period considered for the present work. Overall, the site characteristics (low textural variability, extensive land use) and the experimental setup of the Schäfertal hillslope site provide a rare opportunity to assess the suitability of repeated EMI surveys for mapping soil moisture at the field scale.

2.2 Hydrological characterization

Intensive investigation of the vadose zone water dynamics on the hillslope (Martini et al., 2015) was recently conducted with the aid of a wireless soil moisture and soil temperature monitoring network (*SoilNet*; Bogena et al., 2010). The positions of the 40 measurement nodes of the network (Figure 1) were determined by Weighted Latin Hypercube Sampling with Extremes (wecLHS, Schmidt et al., 2014) using information from geophysical surveys (EMI and gamma-ray spectroscopy) and topographic data. More detailed information can be found in Martini et al. (2015). For each of the network nodes, six sensors were permanently installed in the soil, with two repetitions at three depths (5, 25 and 50 cm), measuring soil moisture and soil temperature with hourly resolution. The sensors in use (*SPADE*, *sceme.de GmbH* i.G., Horn-Bad Meinberg, Germany; Hübner et al., 2009) are based on a ring oscillator. A sensor-specific seven-point-calibration in reference media with well-known dielectric permittivities (Kögler et al., 2013) was conducted to improve the θ measurement accuracy. Additionally, a sensor-specific calibration was performed for the soil temperature sensors. Volumetric soil moisture content was estimated based on the CRIM formula according to Roth et al. (1990), where the dielectric permittivities of soil and air were assumed to be 4.6 and 1, respectively, and the dielectric permittivity of water was calculated based on the measured soil temperature (Kaatze, 2007). Porosity was estimated using volumetric soil samples and ranged between 0.4 and 0.8. More details can be found in Martini et al. (2015).

At each of the 40 sampling locations (Figure 1), the soil profile was described down to the depth of ca. 0.60 m (at the ridgetop, stoniness of the soil due to shallow bedrock limited the investigation to ca. 0.50 m), and the grain size distribution was determined for each node-position and each soil horizon. Four soil topographic units (STUs) were identified: silty loam Cambisols were found on the slopes, with little textural and morphological differences according to the topographic positions. Characteristic hydromorphic features were identified in the valley bottom as indicators of distinct wet state of the loam and silty loam stagnic Gleysols. Here, in winter and spring seasons, soils are frequently water saturated. A summary of soil textural data relevant for the present work is provided in Table 1, additional details of the soil characteristics can be found in Martini et al. (2015).

Hydrol. Earth Syst. Sci. Discuss., doi:10.5194/hess-2016-93, 2016
Manuscript under review for journal Hydrol. Earth Syst. Sci.
Published: 4 March 2016

The hydrological behaviour of the Schäfertal hillslope site was characterized by Martini et al. (2015) using the daily average soil moisture values for each measurement point of the monitoring network at the depths of 5, 25 and 50 cm ($\theta_{d,05}$, $\theta_{d,25}$ and $\theta_{d,50}$, respectively, also named topsoil, intermediate soil horizon and deep soil horizon, as they refer to three distinct soil layers). The monitoring period (from 15 September 2012 to 14 November 2013) comprises different states of soil moisture in response to varying atmospheric conditions (Figure 2). Soil moisture increased during the fall of 2012, when rainfall events were frequent and evapotranspiration (ET) decreased. The winter season was characterized by low precipitation (P) and low ET, followed by the spring season (April to June 2013), dominated by strong dynamics of soil moisture in response to increasing ET and extreme rainfalls up to 49 mm/d. Large areas of Central Europe were flooded at that time, and soils at the Schäfertal site were observed to be saturated in swales and depressions. During the summer period, ET exceeded P and the soil remained drier than the annual mean. The wetting transition started at the beginning of September 2013, with intense rainfalls and decreasing ET.

2.3 Repeated soil-ECa mapping

Soil ECa was measured using an EM38-DD device (*Geonics Ltd.*, Ontario, Canada). The system is composed by two units mounted perpendicularly to each other, both consisting of a transmitter and a receiver coil spaced 1 m. This allows simultaneous measurements of ECa over two depths for every measurement location. The measured data for the two dipole configurations have a different sensitivity response. For the vertical dipole configuration (VDP), this results in a theoretical maximum sensitivity at the depth of ca. 0.40 m and a theoretical maximum investigation depth of ca. 1.50 m at the operating frequency (f) of 14.5 kHz. The sensitivity in the horizontal dipole configuration (HDP, f = 17 kHz) decreases with depth (i.e., maximum sensitivity to very shallow structures), with a theoretical maximum investigation depth of ca. 0.75 m (according to the cumulative sensitivity function by McNeill, 1980).

Surveys were conducted on seven measurement dates within the soil moisture monitoring period (Figure 2), with three measurement dates (19 September, 18 October and 20 November 2012) during the wetting transition; two dates (18 April and 28 May 2013) during the dynamic spring period; and two dates (31 July and 29 August 2013) during the dry summer season. The surveys were conducted with the EMI device mounted on a sledge (made of wood and plastic, in order to avoid conductivity anomalies) at ca. 0.05 m above ground and pulled by one operator at constant walking speed. The study area was divided into three fields: northern slope (i.e., STUs 1 and 2), valley bottom (i.e., STU 3) and southern slope (i.e., STU 4), and each field was measured separately. A fixed location next to the study area (Figure 1), was used as calibration point for instrument nulling (McNeill, 1980) before each survey, and according to the recommendations of, e.g., Robinson et al. (2004), a warm-up period of at least 30 minutes was ensured before measurements were started. Before and after the surveys, ECa was measured along the reference profile (i.e., a fixed 40 m-transect, Figure 1) in order to assess and correct a possible drift in the data (e.g., Sudduth et al., 2001; Abraham et al., 2006). ECa was measured along survey lines spaced ca. 5 m with a rate of 5 records/s, resulting in an approximate resolution of 0.2 m along the main direction. Towards the end of each of the

Hydrol. Earth Syst. Sci. Discuss., doi:10.5194/hess-2016-93, 2016
Manuscript under review for journal Hydrol. Earth Syst. Sci.
Published: 4 March 2016

surveys, crossing lines (Simpson et al. 2009) were measured in order to use the cross-over points for drift correction (CWA 16373, 2011; Delefortrie et al., 2014).

2.4 Processing and integration of time-lapse ECa measurements

Data collected using the HDP configuration showed strong noise. This caused critical problems in data processing and hindered a purposeful data interpretation. As the datasets of ECa measured in VDP did not show significant noise or drift, only those data were used for the present work.

Data points located within a 2-m circular buffer area around each of the soil moisture monitoring network nodes were removed in order to exclude any possible data alteration induced by the magnetic components of the network nodes. By plotting the measured ECa data over time, a limited number of additional outliers could be identified as isolated extreme and unrealistic values.

Data collected with EMI devices may be affected by drift due to instability of the calibration or to temperature changes (Robinson et al., 2004). The measured crossing lines were used to identify and correct the drift: with the help of the interfaces of normal profiles and crossing-lines, a linear drift function was derived for each data set, and used for drift correction. In this step, we assumed that ECa along the reference profile remains constant during the time of survey, i.e., ca. 45 min for the south-facing slope (STU 1 and STU 2 in Figure 1), ca. 15 min for the valley bottom (STU 3) and ca. 30 min for north-facing slope (STU 4).

Due to the sensor nulling performed prior to each survey, a small offset may occur between the data sets collected at different measurement dates, e.g. because of differences in weather conditions which may affect the measurement signal (e.g., Triantafilis et al., 2010). For this reason, we refrain from comparing absolute values from different measurement dates in this study and concentrate on the analysis of differences in spatial patterns of ECa on the individual measurement dates.

ECa data measured along the reference profile within the same day were plotted against time and, if necessary, field-data were corrected by applying a shift based on the mean ECa of the reference profiles. We tested that this did not produce artefacts in the spatial pattern of ECa. Based on the assumption that ECa along the reference profile does not vary within the duration of the measurement (i.e., a few hours), such procedure ensured the data collected with different surveys within the same day to be quantitatively comparable. Measured ECa data were standardized to the reference temperature of 25 °C using the correction factors provided by USDA (1954). Three different reference soil temperatures were calculated (one for the valley bottom and one for each of the two slopes with opposite exposition) averaging all available temperature values measured hourly at the depths of 25 and 50 cm between 9 am and 4 pm on each EMI measurement date (i.e., the time frame in which the surveys were carried out). Except for the topsoil, temperature variations within such time interval are negligible. Among the different measurement dates, the lowest soil temperature was recorded for the EMI survey in November 2012 (i.e., 4 °C in the south-exposed hillslope), and the highest in July 2013 (i.e., 19 °C in the valley bottom).

For each measurement date and for each independent dataset, the experimental variogram was calculated for the temperature corrected ECa and fitted using a linear model for comparability. The fitting parameters were used to spatialize the data using

Hydrol. Earth Syst. Sci. Discuss., doi:10.5194/hess-2016-93, 2016
Manuscript under review for journal Hydrol. Earth Syst. Sci.
Published: 4 March 2016

Hydrology and Earth System Sciences
Discussions

block kriging with a cell size of 1 m. The choice of using linear variogram models was supported by the fact that, despite not all experimental variograms showed a linear behavior at larger lag distances, linear behavior is always given for the 1-m distance used later on for spatialization (data not shown). Afterwards, for each measurement date, the three data sets for the northern slope, the valley bottom, and the southern slope were aggregated, and ECa values of the kriging cell corresponding to the location of each network node were extracted for each measurement date, similar to Zhu et al. (2010). For the following analysis, extracted ECa values (ECa_e) for the seven measurement dates were used in combination with the daily averaged soil moisture (θ_d) at the depths of 5, 25 and 50 cm (based on the available hourly measurements between 9 am and 4 pm) at each single network node for the same measurement dates. For better comparison with the measured ECa, an integrated soil moisture value ($\theta_{d,CS}$) was calculated for every measurement date and for every node of the monitoring network using the cumulative sensitivity function for horizontal coplanar orientation (McNeill, 1980). Although this simple approach neglects vertical changes of soil properties within the soil profile (i.e., soil horizons which may affect the vertical distribution of θ), it can be assumed that the integrated soil moisture values $\theta_{d,CS}$ provide representative information about the weighted θ within the volume of soil sensed by the EMI device.

2.5 Analysis of the temporal stability of soil moisture and ECa patterns

The Spearman rank correlation coefficient was used to investigate the temporal stability of the spatial pattern of ECa_e and θ_d over the seven dates of survey. This coefficient was proposed by Vachaud et al. (1985) as a measure of similarity between two data sets, based on the comparison of the rank of spatially distributed observations between two times, and is defined as:

$$r_s\,(j_1, j_2) = \frac{6\sum_{i=1}^{N}[R(i,j_1)-R(i,j_2)]^2}{(N_s-1)Ns(N_s+1)} \quad (1)$$

where N_s is the total number of spatial observation locations, $R(i,j_1)$ is the rank of the observation for the position i and for the time j_1, and $R(i,j_2)$ is the rank of the observation for the same position, but for the time j_2. The r_s coefficient ranges between -1 and 1, and describes the statistical dependence between the two ranked variables: rs = 1 when there are no changes in the rank of the observations and decreases proportionally to the number of observations for which the rank varies and the number of position changed both toward a higher or lower rank. In other words, the Spearman rank correlation coefficient shows the qualitative similarity between spatially distributed observations.

3 Results and discussion

3.1. Observed spatial patterns of ECa and soil moisture

In contrast to results from other sites (Martinez et al., 2010; Robinson et al., 2012; Lausch et al., 2013; Martini et al., 2013), ECa measured on the Schäfertal hillslope was low ranging between 0 and 24 mSm^{-1} during the complete measurement

Hydrol. Earth Syst. Sci. Discuss., doi:10.5194/hess-2016-93, 2016
Manuscript under review for journal Hydrol. Earth Syst. Sci.
Published: 4 March 2016

period and showed a very small range of spatial variation, which we attribute predominantly to the small variability of soil texture. The range in ECa_e measured along the slopes varied between 7.6 mSm^{-1} in August 2013 and 11.8 mSm^{-1} in November 2013. This small range makes the interpretation of the dynamics in ECa challenging. Nevertheless, the low soil textural variation along the slopes provides the opportunity to evaluate the effect of soil moisture on the measured ECa without the need to account for significant influences of soil texture.

For the seven measurement dates, the overall spatial pattern of measured ECa as well as the extracted apparent electrical conductivity at the positions of the network nodes (ECa_e) showed highest values in the valley bottom (STU 3) and on the footslope (STU 2), whereas the hillslopes (STU 1 and STU 4) showed lower values (Figure 3a-b). Similar spatial patterns were observed for soil moisture (Figure 3c-e) at the three depths of monitoring. Absolute values of ECa vary for the different measurement dates (Figure 3a-b): lowest values were measured in September 2012, May and July 2013, whereas highest ECa was measured in October 2012, April and August 2013.

For the dates of the EMI surveys, the overall spatial distribution of soil moisture measured at the nodes of the monitoring network showed similar distributions (Figure 3c-e), with the lowest θ_d being measured in summit and backslope positions of the south-exposed slope, and highest θ_d in the valley bottom. The topsoil's daily average moisture ($\theta_{d,05}$) exhibited the largest temporal variability, with overall hillslope minimum in September 2012 and July and August 2013 (i.e., 0.15, 0.16 and 0.10 m^3m^{-3}, respectively; Figure 2) and maximum in April and May 2013 (i.e., 0.41 and 0.43 m^3m^{-3}, respectively). Daily average soil moisture of the intermediate soil horizon ($\theta^{d,25}$) ranged between 0.17 (measured in August 2013) and 0.37 m^3m^{-3} (in April and May 2013). The deep soil horizon showed less variable daily average soil moisture ranging between 0.23 and 0.25 m^3m^{-3} except for the measurement dates of April and May 2013 ($\theta_{d,50}$ = 0.35 m^3m^{-3}).

The fact that, during the monitoring period, soil moisture values covered the complete range from very dry (in August 2013) to near-saturation (in May 2013), while little variations were observed in the range and absolute values of ECa for the different measurement dates gives a first, strong indication that, for the Schäfertal hillslope site, soil moisture has little influence on the measured ECa.

3.2 Temporal persistence of the spatial patterns

To further analyse the temporal persistence of the previously observed generally similar spatial patterns in ECa and soil moisture, the Spearman rank correlation coefficient (r_s) was used. To this end, we investigated the temporal persistence of the spatial pattern of ECae as well as the temporal persistence of the spatial pattern of θ_d at the three depths of observation. The overall spatial pattern of ECa_e exhibited a similar trend for all measurement dates (higher values in the valley bottom, lower values on the slopes), whilst the spatial organization of the values within the site showed some differences. Two distinct spatial patterns (Table 2, $r_s \geq 0.9$) of ECa_e were highlighted: one being present in September, October and November 2012 and May 2013, and another one in April, July and August 2013.

The spatial pattern of soil moisture in the topsoil ($\theta_{d,05}$) shows low persistence with r_s decreasing proportionally to the time between two measurement dates (Table 3). The intermediate and deep soil horizons ($\theta_{d,25}$ and $\theta_{d,50}$; Tables 4 and 5) showed a

Hydrol. Earth Syst. Sci. Discuss., doi:10.5194/hess-2016-93, 2016
Manuscript under review for journal Hydrol. Earth Syst. Sci.
Published: 4 March 2016

similar evolution of the pattern, however, as expected, with higher persistence than observed for the topsoil moisture. Three groups ($r_s \geq 0.9$) of spatial distribution could be identified: i) transition from dry to wet state (September, October and November 2012); ii) wet state (April and May 2013); and iii) dry state (July and August 2013).

The direct comparison of the spatial patterns of ECa_e and θ_d showed a clear difference for all three measurement depths. This again supports the observation that, for the Schäfertal hillslope site, soil moisture has little influence on the measured ECa.

3.3. Correlation between ECa and soil moisture at the measurement node positions

Figure 4 shows the relationship between ECa_e and θ_d for the different EMI measurement dates and depths of soil moisture monitoring. The plots in the bottom panels relate ECa_e to the θ values calculated based on the cumulative sensitivity function ($\theta_{d,CS}$) proposed by McNeil (1980). As discussed earlier in the text, intrinsic limitations exist in the EMI measurement technique which may limit the comparability of absolute ECa values; thus we did not attempt to interpret the temporal changes of ECa_e from one measurement date to the other, but rather we focus on the ECa_e-θ_d relationship for every single measurement date and depth of monitoring.

Taking a closer look at the ECa-θ relationship shown in Figure 4, the topsoil moisture ($\theta_{d,05}$) generally showed an overall poor correlation with ECa, with the exception of the survey in April 2013. Nevertheless, the EM38-DD in VDP has little sensitivity to shallow structures (Callegary et al., 2007, 2012; McNeil, 1980). For the depths of 25 and 50 cm, very poor correlation was found during the wetting transition (i.e., September, October and November 2012, with $p > 0.05$) and for May 2013. Better correlation was found for the measurements in April 2013 and in the dry state (July and August 2013). In particular, $R^2 > 0.50$ was found for the ECa_e-θ_d relationship for both the intermediate and the deep soil moisture measurements in April and July 2013, as well as for the 25 cm depth in August 2013. The same is well summarized by the ECa_e-$\theta_{d,CS}$ relationship, as expected. Overall, when the entire hillslope area is considered, ECae was observed to show some correlation with θ_d for only one of the two measurement dates in the wet state and on both measurement dates in the dry state. Nevertheless, no unique correlation between ECa_e and θ_d could be identified for the complete time series which clearly shows that ECa_e cannot always be used as a proxy for quantitative spatial soil moisture distribution at the investigated site.

For most of the cases, measurement points within the same STU clustered within a limited region of the scatter plot to form point clouds, as highlighted by the different colours in Figure 4. This observation supports the concept of STUs, which may facilitate the interpretation of soil moisture and ECa dynamics along the field site. Therefore, useful insights into the factors controlling the temporal dynamics of the ECa_e-θ_d relationship are provided by the relative position of the point clouds of the four STUs, which can be interpreted based on the knowledge of the factors controlling the soil moisture dynamics (gained with the hydrological monitoring as described in Martini et al., 2015) and ECa (from the basic principles already discussed).

For some of the measurement dates, the point clouds of the different STUs occupied different positions relative to each other following changes of ECa and θ, respectively. A distinction, in terms of moisture content, can be observed (Figure 4) between the soils on the slopes (STU 1 and STU 4, south- and north-exposed, respectively, but with similar soil texture), which can be referred to differences of ET on the north and south exposed slopes leading to lower ET and higher soil

Hydrol. Earth Syst. Sci. Discuss., doi:10.5194/hess-2016-93, 2016
Manuscript under review for journal Hydrol. Earth Syst. Sci.
Published: 4 March 2016

moisture values for the north exposed STU4. Such an effect was evident at the beginning of the monitoring period (measurement date in September 2012) as the result of the summer period during which ET is presumed to have led to persistently different moisture values, which remained visible during the rest of the wetting transition (October and November 2012). Similarly, the two measurement dates in the dry season (July and August 2013) show higher θ_d values for STU 4 than for STU 1 at all depths of measurement. ET is also presumed to have had important effects on the topsoil moisture in the valley bottom ($\theta_{d,05}$ blue dots in Figure 4), which has high porosity and remained rather dry in the summer period. This circumstance was inferred as favourable for the occurrence of preferential flow through the topsoil in the valley bottom (STU 3) at the end of the dry seasons in 2012 and 2013 (Martini et al., 2015). Higher θ_d compared to the slopes persisted in the valley bottom during the winter period, due to the combination of local soil properties (i.e. higher porosity), topographic position and presence of a shallow groundwater table. In particular, the latter allowed the soil to reach saturation in the valley bottom, locally, according to the local topographic features. This is evident in Figure 4 for the measurement date in April 2013, represented by five network nodes (out of seven in STU 3, blue dots) which are now well separated from the rest of the data points showing soil moisture values up to 0.72 m^3m^{-3}. At the same time, the groundwater-distant soils on the slopes received water only from snowmelt and from rainfall. The flood event at the end of May 2013 is responsible for the overall high θ_d measured at the site. Large areas within the valley bottom were saturated due to shallow groundwater level, and patches of ponding water were observed; local emergence of return flow was observed at footslope positions within the catchment. In the summer period (measurement dates in July and August 2013 in Figure 4) ET plays an important role in conjunction with local soil properties. Thus, the different moisture content between the soils on opposite slopes (STU 1 and 4) is visible, as well as the higher θ_d in the subsoil in the valley bottom (STU 3).

Based on this, the three distinct spatial patterns of soil moisture observed in Tables 3, 4 and 5 can be attributed to distinct factors: local soil properties and ET in the dry state (July and August 2013); local soil properties, topography and shallow groundwater table in the wet state (April and May 2013); and local soil properties, progressive reduction of ET and progressive rise of groundwater table in the valley bottom during the transition from dry to wet (September, October and November 2012).

In a similar manner, the two distinct spatial patterns of ECa_e (Table 2) can be discussed (Figure 4). Under dry soil conditions (July and August 2013), the higher ECa measured in the valley bottom (STU 3) compared to the slopes can be attributed to the presence of loam and silty loam stagnic Gleysols, with finer texture and high organic matter content. The silty loam Cambisols on the slopes (STU 1, 2 and 4) show similar values of ECa in response to overall similar textural characteristics. In April 2013, an important contribution to the high moisture content on the slopes comes from snowmelt. Thus, a large volume of water within the volume of soil sensed by the EMI device is likely to have low EC_w leading to overall low ECa_e values being comparable to the dry state, when the pores are air-filled. Furthermore, the influence of more conductive water (from groundwater which drains the fertilized agricultural fields of the Schäfertal catchment) enhances the higher ECa_e values for the valley bottom compared to the slopes. This is evident from the gap, in terms of ECa_e, between the blue dots and all other points in Figure 4. As a consequence, the spatial pattern of ECa_e for the measurement date in April 2013 is

Hydrol. Earth Syst. Sci. Discuss., doi:10.5194/hess-2016-93, 2016
Manuscript under review for journal Hydrol. Earth Syst. Sci.
Published: 4 March 2016

substantially similar to the spatial pattern observed in the dry season (Table 2). This is not the case for the measurement date in May 2013, when there was no contribution of water from snowmelt. As a consequence, a higher concentration of ions in the soil solution can be assumed, causing a higher EC_w that is presumed to have contributed significantly to the soil ECa for the entire study area, with the effect of masking the textural differences between the valley bottom and the slopes. Therefore, the spatial pattern of ECa_e for the measurement date in May 2013 does not reflect those of July, August and April 2013. Similarly, the spatial pattern of ECa_e during the wetting transition (September, October and November 2012) is presumed to reflect the contribution of water with different EC_w due to subsurface flow through the soil, where the solid matrix can be enriched with ions due to the process of evaporation and consequent precipitation of ions. Furthermore, the poor correlation between ECa_e and θ_d for the measurement dates in May 2013 and during the wetting transition is determined by the facts that the soil in the valley bottom does not show significantly higher θ_d as compared to the soils on the slopes, as it occurs, instead, for the measurement dates in April, July and August 2013 (Figure 4). This can be explained with the lower θ_d in the topsoil and intermediate soil horizon ($\theta_{d,05}$ and $\theta_{d,25}$, respectively) for the valley bottom (Martini et al., 2015); and with the occurrence of the flood event in May 2013, when the soil reached saturation in large portions of the entire Schäfertal catchment, locally with overland flow. Under such conditions, EC_w can be altered by the flushing of soil organic matter, nutrients and ions released from the solid matrix of the soil from the catchment. Another reason for the different ECa_e patterns observed (measurement dates in September, October, and November 2012 and May 2013, on one hand, and April, July and August 2013, on the other hand, Table 2) lies in the varying relative position of STU 1 and STU 4 along the x-axes (i.e., in terms of ECa). Based on the interpretation discussed above, such differences can be attributed to the occurrence of different water infiltration and transport processes which may take place at different positions according to local soil properties and nonlocal factors such as topography and therefore influence the within-field variability EC_w.

In conclusion, our observations suggest that the spatial pattern of ECa_e (Table 2) represent primarily the spatial variability of soil texture, i.e. higher ECa for the valley bottom (STU 3) than for the slopes (STUs 1, 2 and 4). The occurrence of different hydrological processes (e.g., water infiltration and transport through the vadose zone as well as dynamics of the groundwater level) which take place at different positions along the slope can modify EC_w and, in turn, induce small changes in the ECa pattern. In summary, our observations suggest that soil properties (such as texture, porosity and organic matter content) and, of secondary importance, temporal variations of EC_w, control the spatial pattern of ECa measured with EMI. Soil moisture itself has only a minor effect on ECa, although it is clear that acts as the carrying agent for transporting the ions leading to EC_w.

It is evident from Figure 4 that the range of ECa remained relatively constant for the seven measurement dates although θ varied significantly. The variability of ECa within a single STU was rather small, especially for the soils on the slopes, and the ECa_e-θ_d relationship in Figure 4 is controlled by the relative position of the STUs-clusters. As a consequence, the correlations between ECa_e and θ_d may become more evident when applied to a site with more contrasting soil properties: for instance, if only STU 1 and STU 3 would be considered, for the Schäfertal hillslope site, rather high R^2 values would be found, simply because the two soils show constantly lower ECa_e and lower θ_d, and consistently higher ECa_e and higher θ_d,

Hydrol. Earth Syst. Sci. Discuss., doi:10.5194/hess-2016-93, 2016
Manuscript under review for journal Hydrol. Earth Syst. Sci.
Published: 4 March 2016

respectively. In contrast, if soils with similar texture would be considered (e.g., only the soils on the slopes, excluding the STU 3), no correlation would be found between ECa_e and θ_d throughout the monitoring period, because there are no clear differences in ECa_e among STUs 1, 2 and 4 (Figure 4), and because changes of θ_d do not affect ECa_e, unless they are responsible for significant variations of EC_w. But the latter effect in turn would lead to comparable changes on both slopes.

4 Using EMI for mapping soil moisture and implications for soil mapping

It is widely acknowledged that EMI surveys offer the potential to map the soil spatial variability over large areas within relatively short time, non-invasively and with high spatial resolution (e.g., Doolittle and Brevik, 2014). This makes EMI methods an important aid for optimizing the number of soil samples required to generate a soil map, and for the numerous applications which require detailed soil maps. Results of this study show the importance of repeated surveys in order to capture the dynamics of the spatial pattern of ECa. This, combined with a sound interpretation of the factors controlling such dynamics, allows obtaining the most reliable information from the ECa maps. With respect to that, EMI-based ECa maps can certainly be important supports for hydrological studies, as repeated EMI surveys at one site provide the opportunity to identify stable patterns of soil ECa controlled by the spatial variability of soil properties, which in turn have important effects on the soil water dynamics.

Similar to our findings, Zhu et al., 2010 observed that "wetter sites were generally distributed in the areas with lower elevations, gentler slopes, and depressional landscape positions. These areas also corresponded to a shallower water table and deeper depth to bedrock. These observations suggest that soil ECa is more soil moisture dependent in wetter landscape positions than in drier positions". For the Schäfertal site, the increase in soil EC can be related to two different reasons i) to the wetting of the shallower sections of the soil profile with higher clay content and higher organic matter content (peat soils of the valley bottom) which leads to a release of adsorbed ions from the mineral and organic surfaces and thus releases ions to the soil solution or ii) to the flushing of the valley bottom by groundwater with higher electrical conductivity which also would lead to an increase in soil ECa .

The observed temporal variations of the ECa_e-θ_d relationship showed clearly that soil moisture at the Schäfertal site is not the major control on the measured ECa values, and temporal changes of the ECa pattern are to a large extent unrelated to changes of soil moisture. For EMI measurements conducted at different dates and for different moisture conditions, Farahani et al. (2005) found that higher θ does not necessarily correspond to higher ECa values, which is in good agreement with our observations. Furthermore, Zhu et al. (2010) described that the wetness condition was not the only factor influencing the spatial variability of ECa at their site, and that terrain and soil properties masked the effects of soil moisture on ECa during dry periods, whereas soil ECa was strongly influenced by θ during wetter periods and at wetter locations. Shanahan et al. (2015) found different ECa-θ relationships between a sandy clay loam and a loamy sand, but for both, soil EC decreased with depth, although gravimetric soil water content at depth was higher than or similar to that at the surface.

Hydrol. Earth Syst. Sci. Discuss., doi:10.5194/hess-2016-93, 2016
Manuscript under review for journal Hydrol. Earth Syst. Sci.
Published: 4 March 2016

Referring to the soil equivalent resistance model (Rhoades et al., 1989) on the physical principle behind the ECa measurements, Corwin et al. (2008) discussed the complexity of ECa measurements as being influenced by any soil property or state that influences electrical conductance pathways in soils, and explained that most of the soil properties that influence ECa exhibit co-dependency and thus provide overlapping information on ECa. Furthermore, our data clearly show that the relationship between ECa and a given soil property or state is time-of-measurement dependent, which results from the dynamic nature of e.g. groundwater levels, soil water content and concentration of pore water solution which influence the electrical conductance pathway. This is also confirmed by field data presented in Farahani et al. (2005), and the authors argued that the relationship that they observed between ECa and θ can be partially explained by the dependency of θ on stable soil properties, such as clay content. Furthermore, they showed that such behaviour may produce the effect of magnifying the relationship between ECa and a given soil property at certain times. In the same direction, our results show clearly the difficulties of simply relating ECa to θ. The low variability of soil texture and the rather low clay content at the Schäfertal hillslope site are responsible for the small range of measured ECa.

Corwin et al., 2008 observed that, at sites where dynamic variables (e.g., salinity) dominate the ECa measurement, temporal changes in spatial patterns exhibit more fluidity than systems that are dominated by static properties (e.g., soil texture). Other studies (Zhu et al., 2010; Robinson et al., 2012; Calamita et al., 2015) observed larger spatial variability of soil ECa during the wetter periods and stronger correlation of ECa with clay and topography patterns, and poor spatial organization under dry conditions, supporting the concept of preferred soil moisture states as described in Grayson et al. (1997).

In addition to that, an important aspect to be considered in the interpretation of EMI-based ECa data, are the volume of investigation of the EMI instrument and its spatial sensitivity. Callegary et al. (2007) found that the instrument vertical sensitivity varied significantly with changes in ECa both for homogeneous and heterogeneous soils, although the general shape of all cumulative sensitivity distributions was similar to those predicted by McNeill (1980). According to their results, the depth of investigation indicated by McNeill (1980) holds true only for non-conductive soils, and decreases with increasing ECa. In particular, they reported deviations of 10% or more already at ECa of 3 mSm^{-1}, with depth of investigation reduced to $0.51 \cdot s$ and $0.80 \cdot s$ for the HDP and the VDP configurations, respectively, for the case of the most conductive soil they simulated. In a more recent study (Callegary et al., 2012), the same authors simulated the distribution of the EM field in a 3D space, and demonstrated that the sensitivity pattern has a highly complex shape, including areas of negative contribution (i.e., conductive anomalies may contribute negatively to the instrument ECa reading), and that the HDP- and VDP-volumes of investigation are not as different as assumed from previous studies, although depth-sensitivity functions are different. This implies that caution is required when the ECa data are to be used quantitatively, as the volume of soil sensed by the EMI device may change spatially and temporally. Such an effect may not be a severe limitation for the Schäfertal site, where ECa is low, but may be significant for sites with higher ECa or with more contrasting soil textures.

Given the complexity of the EM field propagation through natural soils (hence, with a certain degree of heterogeneity) any quantitative interpretation of ECa data (e.g. for estimating θ or solute concentration) is difficult to prove with field data from EMI measurements only. In fact, for every point in space where EMI measurements are conducted, measured ECa resembles

Hydrol. Earth Syst. Sci. Discuss., doi:10.5194/hess-2016-93, 2016
Manuscript under review for journal Hydrol. Earth Syst. Sci.
Published: 4 March 2016

the bulk conductivities of all sources contributing to ECa. These are EC_s, and EC_w for the actual volume of investigation of the EMI sensor, which changes according to variations in the electrical conductivity profile. The water itself does not contribute to the soil EC. However, it is the carrying agent for ions released into the pore water, and it is responsible for the thickness of water films around the minerals which themselves control the mobility of ions therein and, consequently affect soil EC (Friedman, 2005).

The interdisciplinary combination of expertise and the use of well-constrained numerical models can certainly improve our ability to extract reliable information from EMI-based ECa datasets. This is not trivial, and involves the fields of pedology, hydrology, soil physics, soil chemistry, and geophysics, as it must account for the propagation of the EM field through the heterogeneous soil material, where complex interactions between stable soil properties and transient state variables take place and are spatially and temporally variable. Furthermore, such models need to be trained with time series of highly resolved spatial data.

Benefits to the use of EMI-based ECa data may arise from the use of multi-configuration EMI systems and calibration procedures, as they allow collecting ECa data from multiple depths at the same time which can be calibrated using profiles of electrical resistivity (e.g., von Hebel et al., 2014; Shanahan et al., 2015). Nevertheless, such procedure is based on the sensitivity function proposed by McNeill (1980), of which the limits of applicability were discussed already. In addition to that, as discussed e.g., by Dafflon et al. (2013), EMI and electrical methods face the equivalence problem, as various combinations of soil structures (in terms of layer boundaries) and EC depth profiles can lead to the same instrument response. Similar considerations are valid for multi-frequency EMI sensors. Tromp-van Meerveld and McDonnell (2009) could not resolve the θ depth profile using an EMI sensor comprising six frequencies, which provided similar responses for six different frequencies although the distribution of θ with depth was non-uniform due to rain events. The study of Calamita et al. (2015) showed similar limitations, and the authors highlighted that a number of factors can make the interpretation of ECa data with respect to θ challenging, and that the use of the EMI method for hydrological applications can be better understood when considering the effects of EC_w and clay minerals.

Shanahan et al. (2015) remarked that in ECa-θ studies it is commonly assumed that a change in soil EC is simply due to a change in the volume of the fluid. Nevertheless their study showed that, under certain circumstances, changes in EMI-based ECa may be confounded by increased EC_w and less closely associated with changes in θ. Cassiani et al. (2015) remarked the need for more consideration for EC_w, which may play an important role. Our study confirms this, at least for the case of low conductive soils, and shows that the large changes of θ at the Schäfertal site have negligible effects on the measured ECa. Different results may be found for different soil types. In fact, larger ECa response to changes in θ was observed for clay-rich soils (e.g., Martinez et al., 2010; Robinson et al., 2012; Shanahan et al., 2015).

Our results apply to the Schäfertal site and to landscapes with similar soil characteristics (low conductive silty loam soils evolved on loess deposits are widespread over large areas of Central and Northern Europe) and calls for proper interpretation of ECa, which is a complex physicochemical property, due to the complex nature of soil. To this end, an interdisciplinary

Hydrol. Earth Syst. Sci. Discuss., doi:10.5194/hess-2016-93, 2016
Manuscript under review for journal Hydrol. Earth Syst. Sci.
Published: 4 March 2016

approach combining pedological and hydrological expertise with solid understanding of the (geo)physical principles underlying the EMI method may certainly improve the results of future studies.

5 Summary and conclusions

Repeated EMI surveys were conducted on a hillslope site within the Schäfertal catchment, of which soil properties and soil moisture dynamics were known. Soil ECa was mapped on seven dates with different soil moisture states, comprising dry, wet and transition from dry to wet. This allowed investigating the effects of θ on the measured ECa under field conditions and provided the opportunity to discuss the physical principles behind EMI measurements of ECa.

Although the range of θ variations was very large throughout the monitoring period, ECa showed a very small range of variation. Temporal changes in spatial patterns of ECa were found to differ from temporal changes in spatial patterns of θ. The observations discussed in the present work support the conclusion that soil moisture is not the major control on ECa measured with EMI, which is, indeed, controlled by a number soil properties and states with a variable and time-varying relative contribution. It is worth remarking that time series data have the potential to reveal the limits of applicability of the EMI method with respect to the specific site conditions and to avoid overinterpretation of geophysical proxies.

Comparing repeated EMI measurements with high-resolution monitoring of soil water dynamics in the vadose zone allowed us to identify two distinct spatial patterns of ECa; the one representing the actual spatial variability of soil properties, i.e., under dry conditions (July and August 2013) or when EC_w was low (April 2013); the other, when different processes, such as water infiltration and transport through the soil and dynamics of the groundwater from the catchment, modify EC_w and, in turn, add to the signal from the stable pattern of soil properties (e.g., in September, October and November 2012 and May 2013). Furthermore, our observations suggest that for soils with low clay content, electrical conductivity of the soil solution rather than the volumetric soil water content may be the factor controlling the temporal variability of ECa.

The combination of repeated EMI measurements and distributed soil moisture monitoring at one site enabled us to provide a process based interpretation of the relationship between ECa measured with EMI and soil moisture, beyond the limits which we might be subject to if only one method would be available.

Acknowledgments

This research has received funding from ExpeER, a project funded by the European community's Seventh Framework programme and the Helmholtz Alliance EDA – Remote Sensing and Earth System Dynamics, through the Initiative and Networking Fund of the Helmholtz Association, Germany. In addition, it was supported by TERENO (TERrestrial ENvironmental Observatories) and by WESS – Water and Earth System Sciences Competence Cluster (Tübingen, Germany). Edoardo Martini acknowledges the support of HIGRADE, the Helmholtz Interdisciplinary Graduate School for Environmental Research. We gratefully acknowledge Mr. S. Gerlach (Agrargenossenschaft Straßberg-Siptenfelde), who

provided access to the site and logistical support, and the colleagues who helped conducting the EMI surveys. Data will be made available to all interested researchers upon request.

References

Abdu, H., Robinson, D.A., Seyfried, M., Jones, S.B., 2008. Geophysical imaging of watershed subsurface patterns and prediction of soil texture and water holding capacity. Water Resour. Res. 44 (4).

Abraham, J.D., M. Deszcz-Pan, D.V. Fitterman, and B.L. Burton (2006), Use of a handheld broadband EM induction system for deriving resistivity depth images, Symposium on the Application of Geophysics to Engineering and Environmental Problems, pp. 1782–1799.

Al-Gaadi, K., 2012. Employing electromagnetic induction techniques for the assessment of soil compaction. Am. J. Agric. Biol. Sci. 4, 425–434.

Altdorff, D., Bechtold, M., van der Kruk, J., Vereecken, H., Huisman, J.A., 2016, Mapping peat layer properties with multi-coil offset electromagnetic induction and laser scanning elevation data, Geoderma, 261, 178-189, doi:10.1016-/j.geoderma.2015.07.015.

Binley, A., Hubbard, S.S., Huisman, J.A., Revil, A., Robinson, D.A., Singha, K., Slater, L.D., 2015. The emergence of hydrogeophysics for improved understanding of subsurface processes over multiple scales. Water Resour. Res. 51. http://dx.doi.org/10.1002/2015WR017016.

Bogena, H., M. Herbst, J.A. Huisman, U. Rosenbaum, A. Weuthen, and H. Vereecken. 2010. Potential of wireless sensor networks for measuring soil water content variability. Vadose Zone J.l 9:1002-1013. doi:10.2136/vzj2009.0173

Borchardt, D. (1982), Geoökologische Erkundung und hydrologische Analyse von Kleineinzugsgebieten des unteren Mittelgebirgsbereichs, dargestellt am Beispiel der oberen Selke, Harz (In German.), Petermanns Geographische Mitteilungen 82(4), 251-262.

Calamita, G., A. Perrone, L. Brocca, B. Onoratic S. Manfreda. 2015. Field test of a multi-frequency electromagnetic induction sensor for soil moisture monitoring in southern Italy test sites, J. of Hydrology. http://dx.doi.org/10.1016/j.jhydrol.2015.07.023

Callegary, J.B., Ferré, T.P.A., Groom, R.W., 2007. Vertical spatial sensitivity and exploration depth of low-induction-number electromagnetic induction instruments. Vadose Zone J. 6 (1), 158. http://dx.doi.org/10.2136/vzj2006.0120.

Callegary, J.B., Ferré, T.P.A., Groom, R.W., 2012. Three-dimensional sensitivity distribution and sample volume of low-induction-number electromagnetic induction instruments. Soil Sci. Soc. Am. J. 76 (1). http://dx.doi.org/10.2136/sssaj2011.0003.

Cassiani G., J. Boaga, M. Rossi, G. Fadda, M. Putti, B. Majone, A. Bellin, 2015, Soil-plant interaction monitoring: small scale example of an apple orchard in Trentino, North Eastern Italy, Science of the Total Environment, doi: 10.1016/j.scitotenv.2015.03.113

CEN Workshop Agreement (CWA) 16373 (2011), Best practice approach for electromagnetic induction (EMI) measurements of the near surface, CEN, p. 56, Brussels, Belgium.

Corwin, D. L., and S. M. Lesch (2005). Apparent soil electrical conductivity measurements in agriculture, Comput. Electron. Agric., 46(1–3), 11–43.

Corwin, D.L., S.M. Lesch, and H. Farahani (2008), Theoretical insight on the measurement of soil electrical conductivity. In: B.J. Allred, J.J. Daniels and M.R. Ehsani (editors) Handbook of Agricultural Geophysics, CRC Press. Boca Raton, FL. Chapter 4 pp: 59-83.

Delefortrie, S., P. De Smedt, T. Saey, E. Van De Vijver, and M. Van Meirvenne (2014), An efficient calibration procedure for correction of drift in EMI survey data, Journal of Applied Geophysics, 110, 115-125, doi: 10.1016/j.jappgeo.2014.09.004.

Doolittle, J., Petersen, M., Wheeler, T., 2001. Comparison of two electromagnetic induction tools in salinity appraisals. J. Soil Water Conserv. 56 (3), 257–262.

Doolittle, J.A., and E.C. Brevik (2014), The use of electromagnetic induction techniques in soils studies, Geoderma, 223–225, 33–45, doi:10.1016/j.geoderma.2014.01.027.

Dafflon, B., Hubbard, S.S., Ulrich, C., Peterson, J.E., 2013. Electrical conductivity imaging of active layer and permafrost in an Arctic ecosystem, through advanced inversion of electromagnetic induction data. Vadose Zone J. 12 (4).

El-Qady, G., Metwaly, M., Khozaym, A., 2014. Tracing buried pipelines using multi frequency electromagnetic. NRIAG J. Astron. Geophys. 3 (1), 101–107. http://dx.doi.org/10.1016/j.nrjag.2014.06.002.

Farahani, H.J., G.W. Buchleiter, and M.K. Brodahl (2005), Characterization of apparent soil electrical conductivity variability in irrigated sandy and non-saline fields in Colorado, American Society of Agricultural Engineers, 48(1), 155−168.

Friedman, S.P., 2005. Soil properties influencing apparent electrical conductivity: a review. Comput. Electron. Agric. 46 (1), 45–70.

Grayson, R.B., A.W. Western, F.H.S. Chiew, and G. Blöschl. 1997. Preferred states in spatial soil moisture patterns: Local and non-local controls. Water Resour. Res. 33:2897–2908. doi:10.1029/97WR02174

Hübner, C., R. Cardell-Oliver, R. Becker, K. Spohrer, K. Jotter, and T. Wagenknecht. 2009. Wireless soil moisture sensor networks for environmental monitoring and vineyard irrigation. In: 8th International Conference on Electromagnetic Wave Interaction with Water and Moist Substances (ISEMA 2009), Helsinki, Finland. pp.408–415.

Kaatze, U. 2007. Reference liquids for the calibration of dielectric sensors and measurement instruments. Measurement Science and Technology, vol.18, pp. 967-976, 2007.

Kögler, S., F. Schmidt, E. Martini, J. Bumberger, S. Zacharias, and U. Wollschläger. 2013. Comparison of two calibration approaches for low-cost soil moisture sensors. In: 7th CMM Conference 2013 Innovative Feuchtemessung in Forschung und Praxis, Krlsruhe, Germany, 24th September 2013.

James, I.T.,Waine, T.W., Bradley, R.I., Taylor, J.C., Godwin, R.J., 2003. Determination of soil type boundaries using electromagnetic induction scanning techniques. Biosyst. Eng. 86 (4), 421–430.

Lausch, A., S. Zacharias, C. Dierke, M. Pause, I. Kühn, D. Doktor, P. Dietrich, and U. Werban, (2013), Analysis of vegetation and soil patterns using hyperspectral remote sensing, EMI, and gamma-ray measurements, Vadose Zone J., 12 (4), doi: 10.2136/vzj2012.0217.

Lück E., Gebbers R., Ruehlmann J. and Spangenberg U. (2009), Electrical conductivity mapping for precision farming. Near Surf. Geophys., 7, 15-25.

Martinez, G., Vanderlinden, K., Ordóñez, R., Muriel, J.L., 2009. Can apparent electrical conductivity improve the spatial characterization of soil organic carbon? Vadose Zone J. 8 (3), 586–593.

Martinez, G., K. Vanderlinden, J.V. Giraldez, A.J. Espejo, and J.L. Muriel, (2010), Field-scale soil moisture pattern mapping using electromagnetic induction, Vadose Zone J., 9, 871–881. doi:10.2136/vzj2009.0160.

Martini, E., C. Comina, S. Priori, and E.A.C. Costantini, (2013), A combined geophysical-pedological approach for precision viticulture in the Chianti hills, Bollettino di Geofisica Teorica ed Applicata, 54(2), 165-181, doi:10.4430/bgta0079.

Martini E., U. Wollschläger, S. Kögler, T. Behrens, P. Dietrich, F. Reinstorf, K. Schmidt, M. Weiler, U. Werban, and S. Zacharias, (2015), Spatial and Temporal Dynamics of Hillslope-Scale Soil Moisture Patterns: Characteristic States and Transition Mechanisms, Vadose Zone J., 14(4), doi:10.2136/vzj2014.10.0150.

McCutcheon, M.C, H.J. Farahani, J.D. Stednic, G.W. Buchleiter and T.R. Green. 2006. Effect of soil water on apparent soil electrical conductivity and texture relationships in a dryland field. Biosyst Engng. 94:19-32

McNeill, J.D. (1980), Electromagnetic terrain conductivity measurement at low induction numbers, Tech. Note TN-6, Geonics Ltd., Mississauga, ON, Canada.

Ollesch, G., Y. Sukhanovski, I. Kistner, M. Rode, and R. Meissner, (2005), Characterization and modelling of the spatial heterogeneity of snowmelt erosion, Earth Surf. Process. Landforms, 30, 197–211, doi:10.1002/esp.1175.

Priori, S., E. Martini, M.C. Andrenelli, S. Magini, A.E. Agnelli, P. Bucelli, M. Biagi, S. Pellegrini, and E.A.C. Costantini (2013), Improving wine quality through harvest zoning and combined use of remote and soil proximal sensing, Soil Sci. Soc. Am. J., 77, 1338-1348, doi:10.2136/sssaj2012.0376.

Pütz, Th., Kiese, R., Zacharias, S., Bogena, H., Priesack, E. Wollschläger, U., Schwank, M., Papen, H., von Unold, G., Vereecken, H. (2011), TERENO-SOILCan - Ein Lysimeter Netzwerk in Deutschland. Proceedings 14. Gumpensteiner Lysimetertagung 2011, 5-10. (in German).

Reinstorf, F. (2010a), Schäfertal, Harz Mountains, Germany. Poster. In: Schumann, S., B. Schmalz, H. Meesenburg, and U. Schröder (editors), "Status and Perspectives of Hydrology in Small Basins, Results and reccommendations of the International Workshop in Goslar-Hahnenklee, Germany 2009, and Inventory of Small Hydrological Research Basins", 30 March – 2 April 2009, Goslar-Hahnenklee, Germany.

Reinstorf, F., J. Tiedke, J. Bauspiess, H. John, and G. Ollesch (2010b), Time series modelling in the Schefertal catchment in the Lower Harz Mountains, central Germany, Proceedings of the Workshop "Status and Perspectives of Hyrology in Small Basins", 30 March – 2 April 2009, Goslar-Hahnenklee, Germany, IAHS Publ. 336.

Rhoades, J.D., N.A. Manteghi, P.J. Shouse, and W.J. Alves, (1989), Soil electrical conductivity and soil salinity: new formulations and calibrations, Soil Sci. Soc. Am. J., 53, 433–439.

Robinson, D.A., I. Lebron, S.M. Lesch, P. Shouse, (2004), Minimizing drift in electrical conductivity measurements in high temperature environments using the EM-38, Soil Sci. Soc. Am. J., 68, 339–345.

Robinson, D., H. Abdu, I. Lebron, and S. Jones, (2012), Imaging of hill-slope moisture wetting patterns in a semi-arid oak savanna catchment using time-lapse electromagnetic induction. J. of Hydrology, 416-417, 39-49, doi: 10.1016/j.jhydrol.2011.11.034.

Roth, K., R. Schulin, H. Flühler, and W. Attinger. 1990. Calibration of time domain reflectometry for water content measurement using a composite dielectric approach. Water Resour. Res. 26:2267–2273. doi10.1029/WR026i010p02267

Saey, T., D. Simpson, H. Vermeersch, L. Cockx, and M. Van Meirvenne. 2009. Comparing the EM38-DD and Dualem-21S sensors to depth-to-clay mapping. Soil Sci. Soc. Am. J. 73:7–12. doi:10.2136/sssaj2008.0079

Sauer, M. C., Jr., Southwick, P. F., Spiegler, K. S. and Wyllie, M.R.J. 1955. Electrical conductance of porous plugs: Ion exchange resin-solution systems: Ind. Eng. Chem. 47, 2187-2193.

Schmidt, K., T. Behrens, J. Daumann, L. Ramirez-Lopez, U. Werban, P. Dietrich, and T. Scholten, (2014), A comparison of calibration sampling schemes at the field scale, Geoderma, 232-234, 243-256, doi: 10.1016/j.geoderma.2014.05.013.

Scudiero, E., Corwin, D.L., Wienhold, B.J., Bosley, B., Shanahan, J.F., and Johnson, C.K.: Downscaling Landsat 7 canopy reflectance employing a multi soil sensor platform. Precision Agriculture. doi: 10.1007/s11119-015-9406-9, 2015.

Shanahan, P.W., A. Binley, W. R. Whalley, and C.W. Watts, (2015), The Use of Electromagnetic Induction to Monitor Changes in Soil Moisture Profiles beneath Different Wheat Genotypes, Soil Sci. Soc. Am. J., 79, 459–466, doi:10.2136/sssaj2014.09.0360.

Simpson, D., M. Van Meirvenne, T. Saey, H. Vermeersch, J. Bourgeois, A. Lehouck, L. Cockx, and U.W.A. Vitharana, (2009), Evaluating the multiple coil configurations of the EM38DD and DUALEM-21S sensors to detect archaeological anomalies, Archaeol. Prospect., 16, 91–102.

Sudduth, K.A., Drummond, S.T., Kitchen, N.R., 2001. Accuracy issues in electromagnetic induction sensing of soil electrical conductivity for precision agriculture. Comput. Electron. Agric. 31 (3), 239–264. http://dx.doi.org/10.1016/S0168-1699(00)00185-X.

Sudduth, K.A., N.R. Kitchen, W.J. Wiebold, W.D. Batchelor, G.A. Bollero, and D.G. Bullock, (2005), Relating apparent electrical conductivity to soil properties across the north-central USA. Comput. Electron. Agric., 46, 263–283, doi:10.1016/j.compag.2004.11.010.

Triantafilis, J., Lesch, S.M., La Lau, K., Buchanan, S.M., 2009. Field level digital mapping of cation exchange capacity using electromagnetic induction and a hierarchical spatial regression model. Aust. J. Soil Res. 47, 651–663.

Triantafilis J., Laslett G.M. and McBratney A.B. 2000. Calibrating an electromagnetic induction instrument to measure salinity in soil under irrigated cotton. Soil Science Society of America Journal 64, 1009–1017.

Tromp-van Meerveld, H.J., McDonnell, J.J., 2009. Assessment of multi-frequency electromagnetic induction for determining soil moisture patterns at the hillslope scale. J. Hydrol. 368 (1), 56–67.

U.S.D.A., (1954), Diagnosis and improvement of saline and alkaline soils, U.S.D.A. Agricultural Handbook 60, by L.A. Richards (editor), U.S. Govt. Print. Off., Washington, D.C.

Vachaud, G.A., A. Passerat de Silans, P. Balabanis, and M. Vauclin, (1985), Temporal stability of spatially measured soil water probability density function, Soil Sci. Soc. Am. J., 49, 822–828, doi: 10.2136/sssaj1985.03615995004900040006x.

von Hebel, C., Rudolph, S., Mester, A., Huisman, J.A., Kumbhar, P., Vereecken, H., van der Kruk, J., 2014. Three-dimensional imaging of subsurface structural patterns using quantitative large-scale multiconfiguration electromagnetic induction data. Water Resour. Res. 50 (3), 2732–2748.

Weller, U., Zipprich, M., Sommer, M., Zu Castell, W., Wehrhand, M., 2007. Mapping clay content across boundaries at the landscape scale with electromagnetic induction. Soil Sci. Soc. Am. J. 71 (6), 1740–1747.

Western, A.W., Zhou, S.L., Grayson, R.B., McMahon, T.A., Blöschl, G., Wilson, D.J. 2003. Spatial correlation of soil moisture in small catchments and its relationship to dominant spatial hydrological processes. J. Hydrol. 286 (1–4), 113–134.

Werban, U., K. Kuka, and I. Merbach, (2009), Correlation of electrical resistivity, electrical conductivity and soil parameters at a long-term fertilization experiment, Near Surface Geophysics, 7(1), 5-14, doi: 10.3997/1873-0604.2008038.

Wollschläger, U., S. Attinger, D. Borchardt, M. Brauns, M. Cuntz, P. Dietrich, J.H. Fleckenstein, K. Friese, J. Friesen, A. Hildebrandt, G. Jäckel, N. Kamjunke, K. Knöller, S. Kögler, O. Kolditz, R. Krieg, R. Kumar, A. Lausch, M. Liess, A. Marx, R. Merz, C. Mueller, A. Musolff, H. Norf, C. Rebmann, F. Reinstorf, M. Rode, K. Rinke, L. Samaniego, M. Vieweg, H.-J. Vogel, M. Weitere, U. Werban, M. Zink, S. Zacharias. Submitted. The Bode Catchment as part of the TERENO Harz/Central German Lowland Observatory: A platform for integrated, interdisciplinary eco-hydrological research. Submitted to Env. Earth Sci.

Zacharias, S., H. Bogena, L. Samaniego, M. Mauder, R. Fuß, T. Pütz, M. Frenzel, M. Schwank, C. Baessler, K. Butterbach-Bahl, O. Bens, E. Borg, A. Brauer, P. Dietrich, I. Hajnsek, G. Helle, R. Kiese, H. Kunstmann, S. Klotz, J.C. Munch, H. Papen, E. Priesack, H.P. Schmid, R. Steinbrecher, U. Rosenbaum, G. Teutsch, and H. Vereecken, (2011), A network of terrestrial environmental observatories in Germany, Vadose Zone J., 10(3), 955-973, doi:10.2136/vzj2010.0139.

Zhu Q., H. Lin, and J. Doolittle, (2010), Repeated Electromagnetic Induction Surveys for Determining Subsurface Hydrologic Dynamics in an Agricultural Landscape, Soil Science Society of America J., 74, 1750-1762, doi:10.2136/sssaj2010.0055.

Tables and captions

Table 1 – Soil texture (median values) of the Schäfertal hillslope site for the topsoil (ca. 0-15 cm) and for the subsoil (ca. 15-60 cm). More detailed information can be found in Martini et al. (2015).

Soil		% Clay	% Silt	% Sand
STU 1	topsoil	17	69	14
	subsoil	15	67	18
STU 2	topsoil	16	78	7
	subsoil	15	79	6
STU 3	topsoil	25	67	10
	subsoil	14	55	28
STU 4	topsoil	15	77	9
	subsoil	13	76	12

Hydrol. Earth Syst. Sci. Discuss., doi:10.5194/hess-2016-93, 2016
Manuscript under review for journal Hydrol. Earth Syst. Sci.
Published: 4 March 2016

Hydrology and Earth System Sciences
Discussions

Table 2 - Spearman rank correlation coefficients (r_s) between spatial patterns of ECa. Values of $r_s \geq 0.9$ are highlighted in bold.

	Sep 2012	Oct 2012	Nov 2012	Apr 2013	May 2013	Jul 2013	Aug 2013
Sep 2012	**1**						
Oct 2012	**0.94**	**1**					
Nov 2012	**0.98**	**0.96**	**1**				
Apr 2013	0.54	0.66	0.60	**1**			
May 2013	**0.95**	**0.94**	**0.93**	0.59	**1**		
Jul 2013	0.55	0.66	0.59	**0.97**	0.58	**1**	
Aug 2013	0.55	0.67	0.61	**0.96**	0.58	**0.98**	**1**

Table 3 - Spearman rank correlation coefficients (r_s) between spatial patterns of soil moisture ($\theta_{d,05}$) in the topsoil. Values of $r_s \geq 0.9$ are highlighted in bold.

	Sep 2012	Oct 2012	Nov 2012	Apr 2013	May 2013	Jul 2013	Aug 2013
Sep 2012	**1**						
Oct 2012	0.85	**1**					
Nov 2012	0.84	**0.95**	**1**				
Apr 2013	0.80	0.73	0.79	**1**			
May 2013	0.73	0.66	0.74	**0.99**	**1**		
Jul 2013	0.67	0.63	0.61	0.67	0.65	**1**	
Aug 2013	0.62	0.54	0.56	0.70	0.70	0.83	**1**

Table 4 - Spearman rank correlation coefficients (r_s) between spatial patterns of soil moisture ($\theta_{d,25}$) in the intermediate soil horizon. Values of $r_s \geq 0.9$ are highlighted in bold.

	Sep 2012	Oct 2012	Nov 2012	Apr 2013	May 2013	Jul 2013	Aug 2013
Sep 2012	**1**						
Oct 2012	**0.97**	**1**					
Nov 2012	**0.95**	**0.99**	**1**				
Apr 2013	0.81	0.81	0.81	**1**			
May 2013	0.80	0.80	0.80	**0.99**	**1**		
Jul 2013	0.86	0.88	0.82	0.80	0.80	**1**	
Aug 2013	0.87	0.88	0.83	0.76	0.76	**0.99**	**1**

Hydrol. Earth Syst. Sci. Discuss., doi:10.5194/hess-2016-93, 2016
Manuscript under review for journal Hydrol. Earth Syst. Sci.
Published: 4 March 2016

Hydrology and Earth System Sciences
Discussions

Table 5 - Spearman rank correlation coefficients (r_s) between spatial patterns of soil moisture ($\theta_{d,50}$) in the deep soil horizon. Values of $r_s \geq 0.9$ are highlighted in bold.

	Sep 2012	Oct 2012	Nov 2012	Apr 2013	May 2013	Jul 2013	Aug 2013
Sep 2012	**1**						
Oct 2012	**0.99**	**1**					
Nov 2012	**0.96**	**0.98**	**1**				
Apr 2013	0.68	0.63	0.65	**1**			
May 2013	0.75	0.73	0.74	**0.97**	**1**		
Jul 2013	0.63	0.82	0.63	0.72	0.69	**1**	
Aug 2013	0.67	0.84	0.65	0.69	0.64	**0.96**	**1**

Hydrol. Earth Syst. Sci. Discuss., doi:10.5194/hess-2016-93, 2016
Manuscript under review for journal Hydrol. Earth Syst. Sci.
Published: 4 March 2016

Figures captions

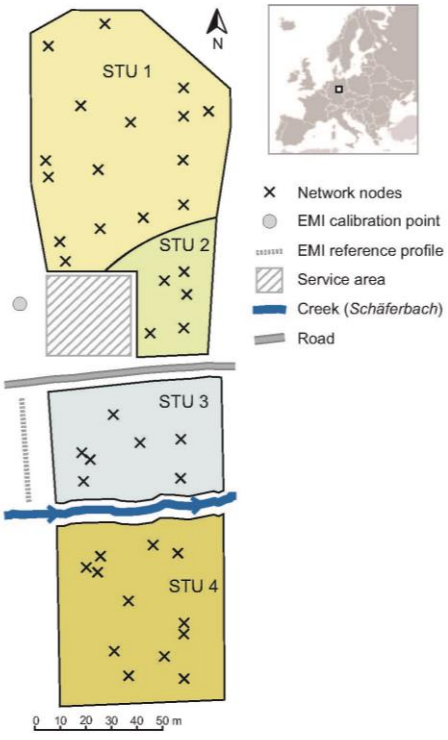

Figure 1- Schematic map of the Schäfertal hillslope site (Martini et al., 2015, modified): the position of the 40 nodes of the wireless soil moisture and soil temperature monitoring network is indicated, as well as the spatial extent of the four soil topographic units (STUs). EMI calibration point (grey dot) and reference profile (dashed line) are indicated in the eastern part of the hillslope.

Hydrol. Earth Syst. Sci. Discuss., doi:10.5194/hess-2016-93, 2016
Manuscript under review for journal Hydrol. Earth Syst. Sci.
Published: 4 March 2016

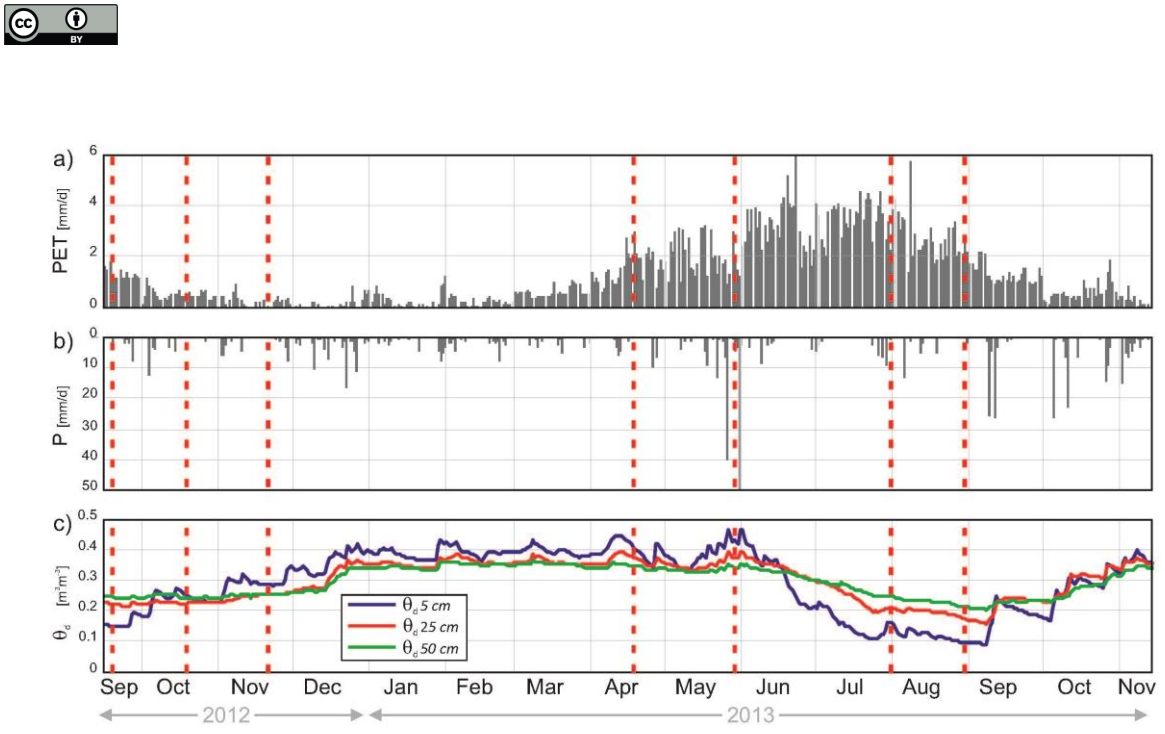

Figure 2 - Time series of a) daily potential evapotranspiration (PET), b) daily cumulative precipitation (P) and c) daily average soil moisture at the three depths of observation ($\theta_{d,05}$, $\theta_{d,25}$ and $\theta_{d,50}$, respectively). Vertical dotted lines indicate the dates of the EMI measurements: 19-Sep-2012, 18-Oct-2012, 20-Nov-2012, 18-Apr-2013, 28-May-2013, 31-Jul-2013 and 29-Aug-2013 (Martini et al., 2015, modified).

Hydrol. Earth Syst. Sci. Discuss., doi:10.5194/hess-2016-93, 2016
Manuscript under review for journal Hydrol. Earth Syst. Sci.
Published: 4 March 2016

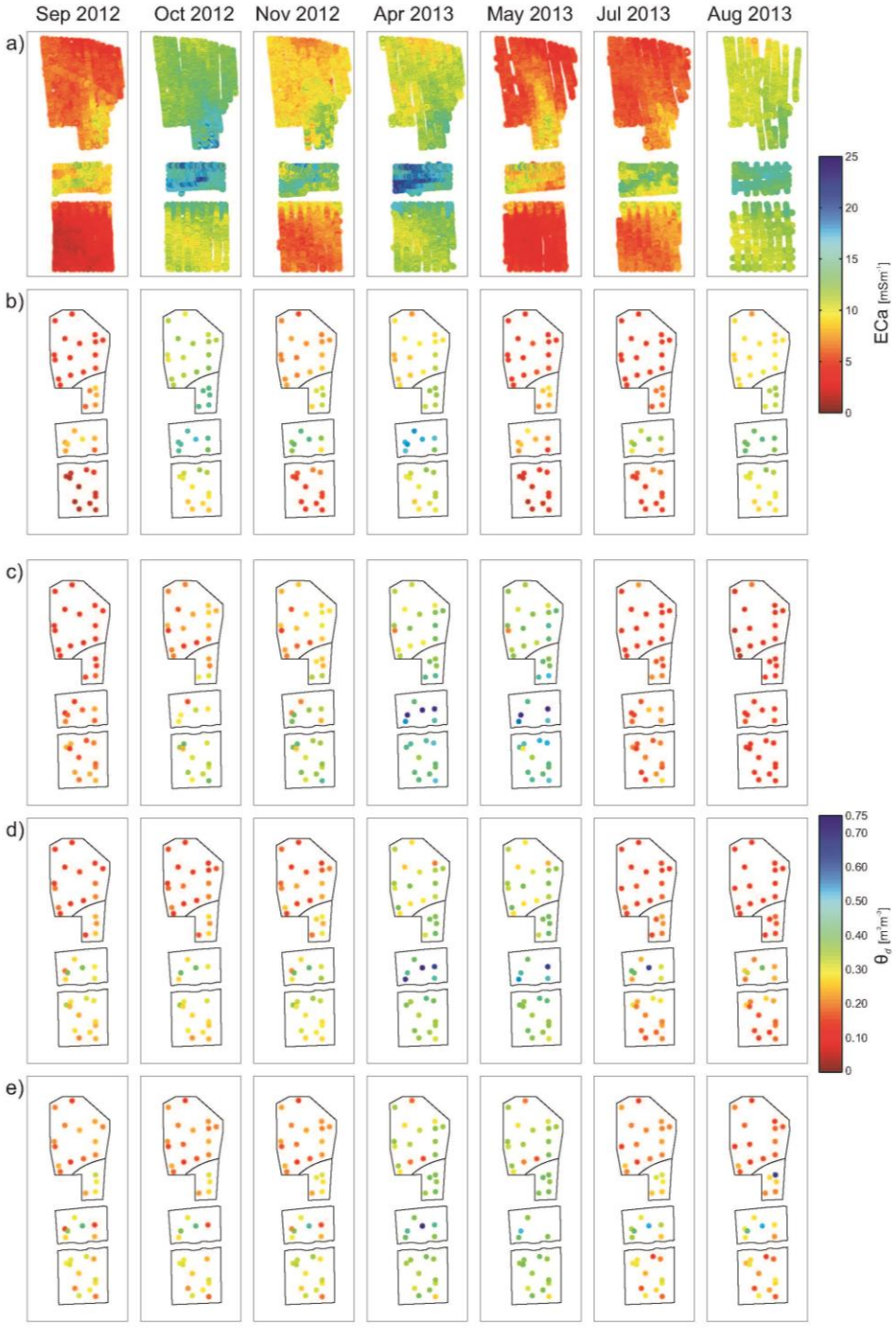

Figure 3- Spatial maps of a) measured ECa (after processing); b) extracted apparent electrical conductivity (ECa_e) for the positions of the 40 nodes of the soil moisture monitoring network; c) daily mean soil moisture at 5 cm ($\theta_{d,05}$); d) daily mean soil moisture at 25 cm ($\theta_{d,25}$); e) daily mean soil moisture at 50 cm ($\theta_{d,50}$).

Hydrol. Earth Syst. Sci. Discuss., doi:10.5194/hess-2016-93, 2016
Manuscript under review for journal Hydrol. Earth Syst. Sci.
Published: 4 March 2016

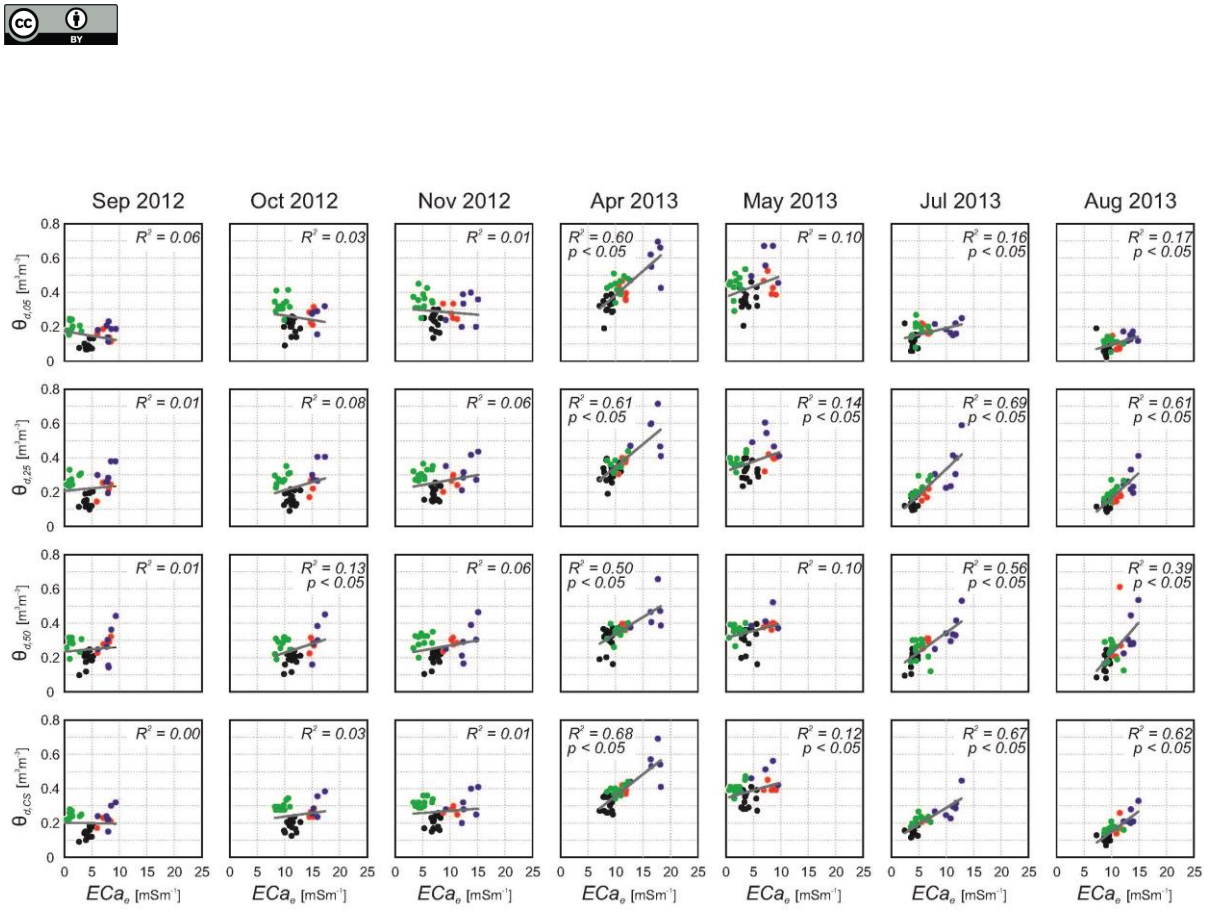

Figure 4 - Linear regression between ECa_e and θ_d for every EMI measurement date and every depth of soil moisture monitoring ($\theta_{d,05}$, $\theta_{d,25}$ and $\theta_{d,50}$, respectively), as well as for the integrated soil moisture calculated using the cumulative sensitivity function ($\theta_{d,CS}$). The different colours represent measurement points located within: STU 1 – black dots; STU 2 – red dots; STU 3 – blue dots; and STU 4 – green dots. Regression coefficients R^2 are reported, as well as the *p*-values, when significant ($p < 0.05$).